EPSC2018

SB14 abstracts

EPSC Abstracts
Vol. 12, EPSC2018-214, 2018
European Planetary Science Congress 2018

Sintering of micrometer-sized water-ice particles

Bastian Gundlach (1) and Judy Ratte (1) and Jürgen Blum (1) and Joachim Oesert (2) and Stanislav N. Gorb (2)
(1) Institut für Geophysik und extraterrestrische Physik, Technische Universität Braunschweig
(2) Zoologisches Institut, Christian-Albrechts-Universität zu Kiel

Abstract

Inside granular materials, the sinter process leads to the growth of a neck between connected particles and, therewith, to an increase of macroscopic physical properties, such as the mechanical strength, or the thermal conductivity of the granular packing. Here, we report on novel experiments conducted to investigate the sinter process of micrometer-sized water-ice particles. Based on the experimental results, we developed a model that is capable to describe the sinter process of granular materials. This model can be used to study icy surfaces of Solar System bodies, such as comets, or icy satellites.

1 Introduction

Sintering is a process that transports material from particles in contact into their neck region. This mass transport is mainly driven by the temperature of the material and by the need of the system to minimize its surface energy. The transport of mass into the neck region leads to an increase of the neck area and, therewith, to an increase of the bonding strength (tensile strength, compressive strength) and of the thermal conductivity of granular materials.

In the context of particle sintering, six material transport mechanisms are known [1]. For water ice under astrophysical conditions (low pressures and temperatures), the vapor transport process, driven by the sublimation of water-ice molecules from the surface of the particles and recondensation of these molecules inside the neck region, is the dominant mechanism [1, 3, 5].

The understanding of the sinter process of small (micrometer-sized) water-ice particles is important to predict the thermal evolution of icy regolith on the surfaces of Solar System objects. Modelling of the sinter process in the context of cometary activity has been carried out [3, 4], but no experiments have ever been performed to study sintering of water-ice under realistic astrophysical conditions.

Fortunately, technical improvements of the cryogenic scanning-electron microscope technique (cryo-SEM) in the past years provides the possibility to study the sinter process in-situ between micrometer-sized water-ice particles.

2 The experiments

The experiments were conducted by observing the neck areas between micrometer-sized water-ice particles with a cryo-SEM (see Fig. 1). The particles were produced by spraying water particles with a pressurized-air driven droplet dispenser directly into liquid nitrogen [2]. After that, the ice particles were transferred into the pre-cooled microscope. Images were taken during the experiment runs to observe the degree of thermal alteration of the ice sample at different temperatures.

The images were analyzed with respect to particle size and sinter-neck size. At the beginning, the sinter

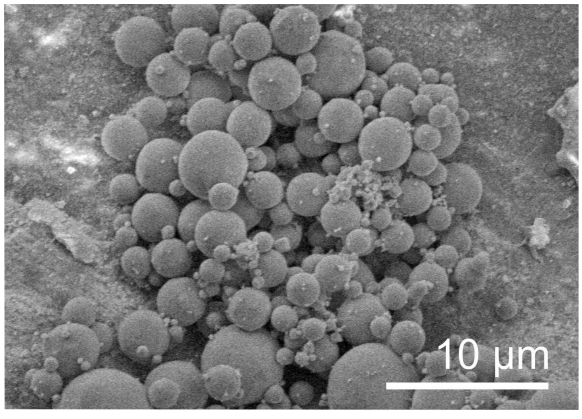

Figure 1: Example of a granular ice sample observed with the cryo-SEM. The acquired images were used to derive the temporal evolution of the sinter neck radii at different (constant) temperatures.

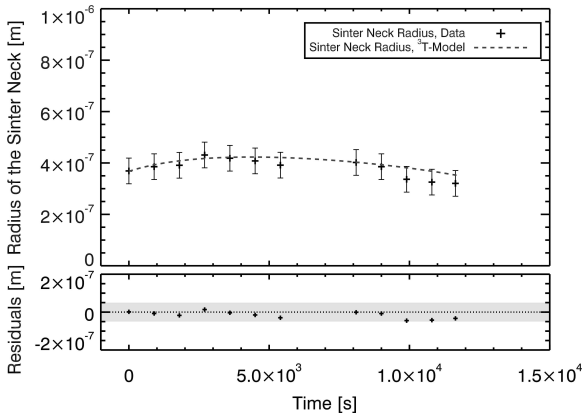

Figure 2: Temporal sinter neck evolution. The pluses are showing the experimental results and the dashed curve visualizes the result of the sinter model. The temperature of the ice samples was 163 K. The bottom panel shows the residuals between measured and modelled data. The gray region around zero denotes one standard deviation error of the measurements.

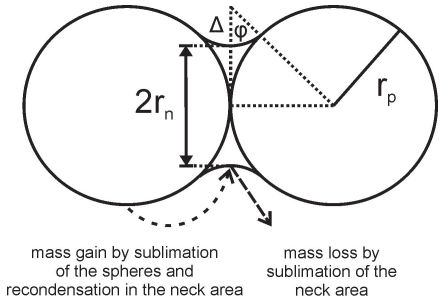

Figure 3: Schematic visualization of the different processes important for the sinter neck evolution of two particles in contact.

process leads to the formation of a neck between the particles (see Fig. 2). However, the formation of the sinter neck is accompanied by mass loss of the particles in contact due to sublimation, with the consequence that the mass transport efficiency decreases. At later stages, the sinter neck shrinks, because sublimation removes more molecules than replenished by the mass transfer.

3 The sinter model

The sinter model developed in the framework of this project is based on three main concepts (see Fig. 3): 1) the mass transport from the particles to the neck region leads to the formation and growth of the sinter neck (classically known as sinter process), 2) sublimation leads to shrinkage of the particles in contact, which decrease the effectiveness of the mass transport into the neck region, and 3) the neck area also loses mass due to sublimation. These three concepts define the basis of the developed sinter model (details can be found in our upcoming paper; Gundlach et al., submitted to MNRAS).

4 Results and Conclusions

Advances in the cryo-SEM technology enabled the possibility to study the sinter process between micrometer-sized water-ice particles. Based on the obtained experimental results, we developed a sinter model that takes, not only the importance of the mass transfer, but also of the sublimation process, into account. This model can be used to study the thermal evolution of icy Solar System objects, such as comets, or icy satellites. Details of the model results will be presented during the EPSC 2018 in Berlin.

Acknowledgements

We acknowledge the DFG for supporting this work (project: GU 1620/1-1).

References

[1] J. R. Blackford: Sintering and microstructure of ice: a review. Journal of Physics D: Applied Physics, 2007, 40, R355-R385.

[2] B. Gundlach and S. Kilias and E. Beitz and J. Blum: Micrometer-sized ice particles for planetary-science experiments - I. Preparation, critical rolling friction force, and specific surface energy. Icarus, 2011, 214, 717-723.

[3] K. J. Kossacki and N. I. Kömle and G. Kargl and G. Steiner: The influence of grain sintering on the thermoconductivity of porous. Planetary and Space Science, 1994, 42, 393-398.

[4] L. Ratke and H. Kochan and H. Thomas: Laboratory studies on cometary crust formation: The importance of sintering. Asteroids, Comets, Meteors, 1991, 497-500.

[5] F. B. Swinkels and M. F. Ashby: A second report on sintering diagrams. Acta Metallurgica, 1981, 29, 259-281.

EPSC Abstracts
Vol. 12, EPSC2018-421-1, 2018
European Planetary Science Congress 2018

An Ultra-Low-Gravity Centrifuge in Low-Earth Orbit

Stephen R. Schwartz[1,*], Erik Asphaug[1], Jekan Thangavelauthum[2], Aman Chandra[2], Ravi teja Nallapu[2], Leonard Vance[2]
[1]Lunar and Planetary Laboratory, University of Arizona, Tucson AZ, [2]Space and Terrestrial Robotics Laboratory (SpaceTREx), Aerospace and Mechanical Engineering, University of Arizona, Tucson AZ, [*]<*srs-at-lpl.arizona.edu*>

Abstract

Near-Earth small bodies such as 162173 Ryugu and 101955 Bennu produce gravity fields around 4 orders of magnitude below that of Earth and their surfaces do not correspond to equipotential surfaces. Still, we observe familiar geologic textures and landforms that are the result of the granular physical processes that take place on their surfaces. However, the nature of these landforms, their origins, and how these surfaces react to interrogation by probes, landers, rovers and penetrators remain largely unknown.

We present the concept of a simple CubeSat-hosted laboratory that consists of a centrifuging chamber of grains in low-Earth orbit as a test-bed to observe granular dynamics in low-gravity environments. We describe the first flight demonstration, where small meteorite fragments will pile up to create a patch of real regolith under realistic asteroid conditions, paving the way for subsequent missions where landing and mobility technology can be flight-proven in the operational environment, generated in low-Earth orbit.

1. Introduction

Much has been learned about small-body geology [1], but for most practical purposes it remains poorly understood. Interacting with its surface therefore presents a risk. Even seemingly straightforward operations present great uncertainty: how does low-gravity regolith respond when interrogated by sampler heads, landing feet, astronaut boots, rover wheels, or excavation tools? Can a spacecraft be anchored to embedded rocks? Are landforms stable, or will exploration or excavation activities disturb them catastrophically?

We are developing AOSAT-1 as a way to quantify how granular materials behave in low-gravity environments [2]. A better understanding is essential to addressing these practical questions of how to appropriately interact with these environments. It also tells us how to interpret what we see in the context of Solar System evolution. How does cohesion affect the interactions between discrete grains? As gravity decreases, some type of cohesion will take over as the dominant force between grains [3] and will greatly influence outcomes from various stresses both quantitatively and qualitatively [4,3,5]. It has also been shown that packing can strongly affect these interactions [6]. In practice, how does packing and porosity influence the response of grains in these environments?

2. Setup

The AOSAT-1 centrifuge chamber will be dedicated to the study of physical phenomena in low gravity. Inserted into low-Earth orbit and filled with granular material, a first, 3-U (10 × 10 × 34 cm) CubeSat, AOSAT-1 (**Fig. 1**), will be launched in 2019 and sent into controlled rotations, simulating the gravitational environment of interest. This will compliment the impending first sample acquisition attempt at Ryugu, which is to take place before solar conjunction this winter [7], as well as future sample acquisition attempts at Ryugu and Bennu [7,8], by helping to explain the regolith response that will be observed.

3. Design

The science payload of AOSAT-1 features internal sensors and optical cameras aimed at a regolith chamber, returning image data for analysis on Earth. Tunable vibrators provide additional experiments, and have the practical benefit of shaking granules off the viewing glass. The spaceflight components (roughly 1U, or 10 × 10 × 10 cm) are positioned at one end of the chassis, and the lab chamber at the other. This positions the center of mass near the 'top' of the chamber (**Fig. 1**), facilitating the separation of engineering requirements: for the spacecraft to function and return data, and for the lab chamber to run experiments and produce data. Experiments include formation of a stable pile at the angle of repose, reversal of torque to create an avalanche, and vibrators to fluidize the regolith. Experiments are conducted in a spun state, lasting minutes to hours; communications with the ground are conducted afterwards, in a de-spun state, tracking the ground station for several orbits. Centrifuge conditions are attained using a single reaction wheel that is capable

of spinning the spacecraft about one of its short axes up to several rotations-per-minute (rpm). The wheel is sized to apply the required torque without saturation. Electromagnetic rods (magnetorquers) are used to stabilize off-axis motions during spin-up. We model this torque in combination with flywheel action and irregular spacecraft mass distribution, to show the dynamical stability of AOSAT-1 (**Fig. 2**). Oscillations damp quickly, so that 1 rpm rotation is stabilized within 15 s, assuming a worst-case mass distribution (the entire regolith pile offset at a far corner of the chamber). We find that after shifts in the regolith mass distribution, AOSAT-1 will stabilize in its experimental mode in minutes [9]. After each experiment, the magnetorquers are used to stop the rotation so that the spacecraft can point and communicate with Earth.

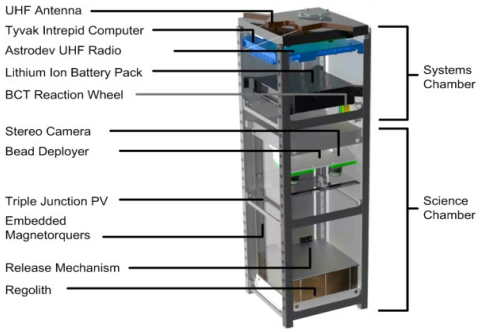

Figure 1: AOSAT-1. The mission will demonstrate an on-orbit centrifuge laboratory to simulate small-body gravity conditions.

4. AOSAT-1 Science

JAXA's Hayabusa-2 mission [7] and NASA's OSIRIS-REx mission [8] are set to perform the most robust to-date experiments involving regolith surfaces in sub-milligravity environments, using sampler heads, and, in the case of Hayabusa-2, a small hypersonic impactor. These missions will obtain images, thermal data, and other measurements indicating the force response. With AOSAT-1, watching simple, but informative granular dynamics play out in a low-gravity environment, without the ops- and risk-related constraints on data-acquisition time, will compliment and help to explain the sample-acquisition data from these small-body sampling missions.

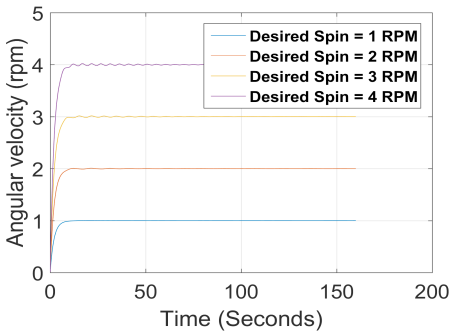

Figure 2: Dynamical stability calculation of AOSAT-1 assuming a worst-case regolith distribution scenario. A single reaction wheel creates a wobble stabilized by magnetorquers.

We will exploit the benefits that come with having a long-term, sustained experiment, including the ability to observe the dynamics inside the chamber continuously for long periods—important given the low velocities and weak forces.

Numerical modeling of granular material will be performed using PKDGRAV [10–13]. This will be of great value in quantifying the material parameters, including static, kinetic, rolling, and twisting frictions [13,14], as well as cohesive properties [5]. These material models can then be applied in large-scale simulations involving small bodies, both for studies of evolutionary processes [15] and for simulating the interrogation of the surface by spacecraft mechanisms [16].

References

[1] Murdoch, N., et al. in *Asteroids IV* **42**, 767 (2015). [2] Asphaug, E., et al. *npj Microgravity* **3**, 16 (2017). [3] Sánchez, P. & Scheeres, D.J. *AIP Conference Proceedings* **1542**, 955 (2013). [4] Schwartz, S.R., et al. *EPSC/AAS-DPS* **41**, 27.11 (2009). [5] Zhang, Y., et al. *ApJ* **857**, 15 (2018) [6] Slotterback, S., et al. *Phys. Rev. E* **85**, 021309 (2012) [7] Tsuda, Y., et al., *Acta Astronaut.* **91**, 356 (2013) [8] Lauretta, D.S., et al. *Space Sci. Rev.* **212**, 925. [9] Nallapu, R., et al. *Adv. Astron. Sci.* **159**, 17–064 (2017). [10] Stadel, J. *Ph.D. Thesis*, U. Washington (2001). [11] Richardson, D.C., et al. *Icarus* **143**, 45 (2000). [12] Richardson, D.C. *Icarus* **212**, 427 (2011). [13] Schwartz et al. *Granular Matter* **14**, 363 (2012). [14] Zhang, Y. et al. *Icarus* **294**, 98 (2017). [15] Yu, Y., et al. *Icarus* **242**, 82 [17] Schwartz, S.R., et al. *Planet. Space Sci.* **103**, 174 (2014).

EPSC Abstracts
Vol. 12, EPSC2018-568, 2018
European Planetary Science Congress 2018

What's Inside a Rubble Pile Asteroid? DISCUS - a Tomographic Twin Radar Cubesat to Find Out

Jakob Deller(1,*), Patrick Bambach(1), Esa Vilenius(1), Sampsa Pursianen(2), Mika Takala(2), Hans Martin Braun(3), Harald Lentz(3), Manfred Wittig(4)

(1) Max Planck Institute for Solar System Research (Justus-von-Liebig-Weg 3, D-37077 Göttingen),
(2) Tampere University of Technology
(3) RST Radar Systemtechnik GmbH
(4) MEW-Aerospace UG, Hameln, Germany
(*Email:deller@mps.mpg.de)

Abstract

DISCUS, the Deep Interior Scanning CubeSat, is a mission concept based on a penetrating step frequency radar to resolve the interior structure of a rubble pile asteroid using computed tomography.

A big fraction of asteroids with d>240 m are suspected to be loose piles of rocks and boulders bound together mainly by gravity and weak cohesion. Still, to date the size and distribution of voids and monolith inside these "rubble-piles" are not known. To perform a full tomographic interior reconstruction a bistatic CubeSat configuration has been investigated by TU Tampere, Radar System Technology (RST) and the Max Planck Institute for Solar System Research (MPS). The concept is based on two 6U CubeSats, both carrying an identical 1U sized stepped frequency radar. As stepped frequency radars can be built compact, require less power and generate less data volume compared to other radar applications they are well-suited for small sat platforms.

In 2017 the Concurrent Design Facility of ESA/ESTEC conducted two studies relevant for DISCUS. In the Small Planetary Probes (SPP) study DISCUS served as a reference payload for a piggyback mission to a NEA or a main belt asteroid. The M-ARGO study investigated a stand-alone mission to a NEA, with a DISCUS sized instrument. Based on the spacecraft design of SPP and M-ARGO we could prove the instrument requirements as feasible and evaluate our science case from the orbits and mission duration that have been identified by the studies.

Using inversion methods developed for medical tomography the data would allow to reconstruct the large scale interior structure of a small body. Simulations have shown that the measurement principle and the inversion method are robust enough to allow full reconstruction of the interior even if the orbits do not cover the entire surface of the asteroid.

The measurement results of the mission will help to gain a better understanding of asteroids and the formation mechanisms of the solar system. In addition, the findings will increase the predictability of asteroid impact consequences on earth and improve future concepts of asteroid deflection.

EPSC Abstracts
Vol. 12, EPSC2018-581, 2018
European Planetary Science Congress 2018

Numerical simulations of a lander's interaction with a low-gravity asteroid regolith surface: application to MASCOT on board Hayabusa2

Florian Thuillet (1), Patrick Michel (1), Clara Maurel (2), Ronald-Louis Ballouz (3,4), Yun Zhang (3,5), Derek C. Richardson (3), Jens Biele (6), Eri Tatsumi (7), Seiji Sugita (7)
(1) Lagrange Laboratory, Université Côte d'Azur, Observatoire de la Côte d'Azur, CNRS, France, (2) Massachusetts Institute of Technology, USA, (3) University of Maryland, USA, (4) Institute for Space and Astronautical Studies, Japan, (5) Tsinghua University, China, (6) DLR German Aerospace Center, Germany, (7) University of Tokyo, Japan

Abstract

We ran a campaign of simulations of Hayabusa2's lander MASCOT impacting the regolith surface of its target asteroid Ryugu, and looked at the outcome for different parameters linked to the characteristics of the impact and of the regolith. The aim is to provide valuable information a posteriori on the regolith properties from data on MASCOT's first impact and to support the landing site selection.

1. Introduction

The JAXA Hayabusa2 sample return mission is currently visiting the C-type near-Earth asteroid Ryugu and will come back to Earth in 2020 with samples. In early October, Hayabusa2 is planed to release the DLR/CNES lander MASCOT (Mobile Asteroid SCOuT) [1] that will perform in-situ investigations of Ryugu's surface. However, since the surface's properties of Ryugu are still poorly constrained, the observation by the cameras onboard Hayabusa2 of the traces left by MASCOT at first impact will provide insightful information about the nature of the regolith and simulations of the impact can help inferring unobserved properties.

We performed hundreds of numerical simulations of MASCOT's low-speed impact on the surface, for different impact and regolith characteristics. The purpose is both to support the landing site selection and finding MASCOT on the asteroid, as well as to expand our knowledge of Ryugu's regolith from the observations of MASCOT's traces.

2. Method

Our simulations were performed with the N-body gravity tree code *pkdgrav*, using a Soft-Sphere Discrete Element Method (SSDEM) to compute interactions between the regolith grains [2]. In our simulations, regolith particles are initially at rest in a 75-cm radius cylinder, under Ryugu's gravity (about 2.5×10^{-4} m s^{-2}). The particle size distribution is assumed to be gaussian with a 1-cm mean radius, a 33% standard deviation sigma, and a cut-off at one sigma. We considered two types of friction between the grains: a moderate friction and a gravel-like one, which differ from their angles of repose, as well as three bed depths (15 cm, 30 cm, and 40 cm). MASCOT is numerically made of "reactive" walls (inertial walls that interact with particles), joined in a 10-kg cuboid with a small prominence representing the spectrometer MicrOmega. The impact speed is set at 19 cm s^{-1}, for three different orientations (landing flat, with its back corner first or with its front one) and five impact angles (from 0 to 60° from the vertical). We analyzed the behavior of MASCOT after the impact, in particular the traveled distance, its speed and spin after impact, and the traces left on the surface after the first bounce, which will be observed from the main spacecraft. These traces are linked to the distance MASCOT will travel and their observations will be valuable for an engineering purpose to deduce MASCOT's final position and a posteriori to deduce regolith properties.

3. Results

3.1. Influence from sensitive parameters

The largest traveled distances as well as the highest outgoing speed and spin are obtained with grazing impacts, with MASCOT landing on its back corner first, on a shallow gravel-like-regolith bed [3].

Moreover, a moderate-friction regolith results in a more homogenous and deeper crater than a gravel-like regolith (see Fig. 1). A back-corner-first orientation

and gravel-like regolith combination leads to a recognizable feature on the ground: a two-hole crater (see Fig. 1).

In order to expand our results to multiple bounces, we also checked the influence of impact speed. We find that the outgoing-to-incoming speed ratio (or coefficient of restitution CoR) seems to change (here, to increase) only for very slow incoming speeds (about 2 cm s^{-1}). As expected, slow impact speeds lead to shallower craters and less pronounced features.

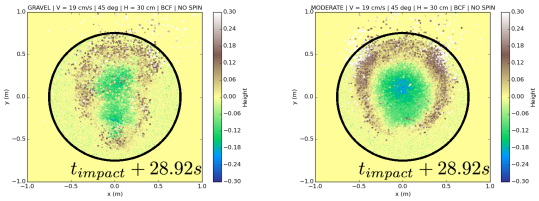

Figure 1: Characteristics of the trace left by MASCOT on the regolith (in cm) 29 s after the impact for gravel-like (left) and moderate-friction regolith (right).

3.2. Presence of a boulder

Since the resolution of Hayabusa2's optical navigation camera may not be able to detect relatively small boulders at the moment of landing site selection, we ran simulations with a grains' aggregate representing a 5-kg boulder in the regolith bed. We found that a boulder buried at a depth of 15 cm in the regolith bed has no big influence on the results presented previously. However a boulder on the surface or just covered by a thin layer of regolith significantly increases the outgoing speed and the stochasticity of the impact. We also checked that buried boulders located on the side of the impact point have no big influence on MASCOT's behavior.

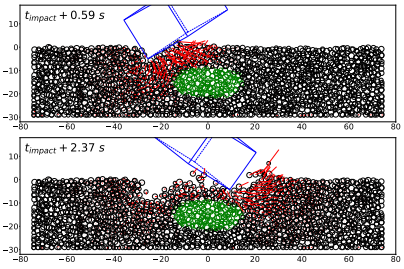

Figure 2: Cross-section snapshots of MASCOT (in blue) impacting the regolith bed, taken 0.59 s and 2.37 s after the impact. Green particles represent the boulder and red lines are particle 2-D projected velocities.

4. Summary and Conclusions

We found that several sensitive parameters play a role on the outcome of the impact, linked to MASCOT's impact geometry or to the regolith characteristics (friction and bed depth). The speed of the impact does not seem to change the CoR whereas it has an expected influence on the depth of the traces and the traveled distance. We are currently running simulations to see the influence of a slope on the impact, as the lander may encounter non-flat surfaces as it repeatedly bounces on the asteroid. We also plan to investigate the influence of a power-law size distribution for the grains and to add cohesion to our model, as well as to compare our results with the real MASCOT impact(s) expected for the beginning of October. This database of simulations will be used to infer regolith properties of Ryugu from MASCOT's traces.

Acknowledgements

F.T. is supported by a PhD fellowship of the University of Nice-Sophia. P.M. and F.T. acknowledge funding support from the French space Agency CNES, as well as from Academies of Excellence: Complex systems and Space, environment, risk, and resilience, part of the IDEX JEDI of the Université Côte d'Azur in connexion with its Center for Planetary Origins (C4PO). Simulations were performed at Mésocentre SIGAMM hosted at the Observatoire de la Côte d'Azur. and on the Deepthought2 HPC cluster at the University of Maryland.

References

[1] Ho, T.M. et al.: MASCOT–The Mobile Asteroid Surface Scout Onboard the Hayabusa2 Mission, Space Science Reviews, Vol. 208, pp. 339-374, 2016

[2] Schwartz, S.R., Richardson D.C., Michel, P.: An implementation of the soft-sphere discrete element method in a high-performance parallel gravity tree-code, Granular Matter, Vol. 14, pp. 363-380, 2012

[3] Thuillet F., Michel P., Maurel C., Ballouz R.-L., Zhang Y., Richardson D.C., Biele J., Tatsumi E., Sugita S.: Numerical modeling of lander interaction with a low-gravity asteroid regolith surface: Application to MASCOT on board Hayabusa2, A&A, in press, 2018

EPSC Abstracts
Vol. 12, EPSC2018-797-1, 2018
European Planetary Science Congress 2018

Studying surface morphologies of comet 67P/C-G using discrete element simulations

D. Kappel (1), K. Otto (1), N. Oklay (1), T. Michalik (1), D. Haack (1), E. Kührt (1), D. Tirsch (1), S. Mottola (1), O. Groussin (2)
(1) German Aerospace Center (DLR), Institute of Planetary Research, Berlin, Germany (david.kappel@dlr.de), (2) Aix Marseille Université, CNRS, Laboratoire d'Astrophysique de Marseille (LAM), Marseille, France

Abstract

We use the discrete element method (DEM) to numerically simulate the surface layer regolith dynamics of comet 67P/Churyumov-Gerasimenko (hereafter 67P/C-G) in order to infer mechanical properties of the surface material.

1. Introduction

Our overarching aim is to investigate the physics of volatile materials of asteroids and comets. To constrain mechanical properties of the surface regolith of comet 67P/C-G, we focus on various morphological features as they have been observed by the Rosetta mission, and aim to reproduce them by DEM modeling of corresponding simulation scenarios. Since the modeling cannot capture the full real-world complexity, the immediate aim is to identify the dominating physical processes involved in the formation of the features and to find a working set of parameters that enables the simulations to be reasonably realistic. The simulation scenarios are then used as starting points for parameter sensitivity studies to constrain mechanical properties, contact forces, particle sizes, etc. of the surface layer material. This is later needed to investigate more complex scenarios like triggers and early phases of outbursts.

2. Numerical modeling

The simulations are implemented using the open source DEM simulator LIGGGHTS [1]. Generally, we assume the surface particles to be represented by poly-disperse spheres consisting of a mixture of dust and water ice. The spheres interact according to the Hertz contact model and additionally are subject to cohesion, friction, rolling friction (also as proxy for more complex particle shapes), and ambient surface acceleration. Furthermore, parallel bonds [2,3] between the spheres can be introduced that break when the inter-particle stresses exceed certain threshold values. This way, we can also model the hard consolidated terrain that was found at many places on the surface and may result from water ice sintering. To better manage the different size scales of the scenarios and save computational resources to enable the simulation of macroscopic scenarios with relatively small grains, we apply a technique called coarse-graining. Here, instead of individual particles we consider computational parcels of several particles. The model parameters have to be suitably scaled to lead to the same energy density, and evolution of energy density, as for the unscaled system of individual particles [4]. Later inclusion of Monte-Carlo-based modeling of sublimation and recondensation of volatiles and Knudsen gas flow through the surface layer will provide us with a tool to research triggers and early phases of outbursts as well as other volatile-related processes.

3. Discussion of scenarios

We consider four different simulation scenarios related to observations on comet 67P/C-G.

Scenario 1 – Boulder Stability. We start with the requirement that boulders of sizes observed on the nucleus surface have to be stable without collapsing under their own weight or when falling from small heights (e.g. cliffs). For this purpose, we assume a large spherical boulder to be made up of small grains and investigate conditions for it to be reasonably stable when dropped from small altitudes above a hard surface. The boulder totally disintegrates when the bonds are set too weak, whereas too strong bonds leave the boulder undamaged. The bond break threshold is varied until a reasonable behavior is obtained (order of 10-30% of the bonds broken after settling). This provides an order-of-magnitude estimate of the bond strength that is related to the water ice content.

Scenario 2 – Cliff Collapse. Cliffs and overhangs are stable, but not so stable as to prevent collapses that indeed have been observed on the nucleus surface [5,6]. We develop a corresponding simulation setup and vary the bond strength starting with Scenario 1 results. Too weak bonds, while allowing low-level seismic shaking to trigger the collapse, prevent the formation of bouldered debris, whereas stronger bonds enable some bonds to survive the fall but prevent collapse just by the seismic activity. In the latter case we have to introduce artificial cracks to trigger the collapse. The post-collapse boulder size distribution and angle of repose provide further constraints on mechanical parameters.

Scenario 3 – Wind-Tails. Wind-tail-like structures and moats have been observed around many exposed boulders [7,8]. We model this scenario by introducing a steady randomized stream of particles colliding with a large obstacle in a small-particle bed. The incoming model grains are set to move at local orbital velocity on inclined, roughly unidirectional trajectories. To avoid boundary effects, the simulation geometry is set to be periodic in the horizontal dimensions. We obtain a slowly rising equilibrium surface resulting from the local balance between erosion by impacting fast grains and deposition of mobilized slow grains. The obstacle shields the erosion, which results in the formation of a 'wind-tail' where deposition predominates erosion. In front of the obstacle, additional erosion by incoming grains reflected at the obstacle can yield a moat. This depends on the shape of the obstacle, the flat front face of a cube being more effective than the rounded shapes of cylinders or spheres that distribute the reflected particles into many directions. Grain sizes, inter-particle forces as well as velocity and inclination of the injected particles affect the equilibrium surface, which enables to infer some of these parameters from observations.

Scenario 4 – Thermal Fractures. Crack polygons have been observed in many places where consolidated material is exposed [9]. They presumably result from stresses induced by spatial and temporal gradients of grain size variations with temperature. For the uppermost surface layers we use an external parameterization of temperature in dependence on depth below the surface and on rotational phase, according to a thermal model for a given surface location and heliocentric distance [10]. We take ice creep into account by first computing the time-dependence of the horizontal internal stress at given depth as solution to the differential equation that results from continuum theory by balancing the temperature dependent elastic, thermal, and viscous strain rates [10]. After many comet rotations, this solution becomes cyclic and independent of the initial value, but to be more efficient we instead retrieve the initial value that starts the periodic solution. The radii of the spheres in a bonded particle bed are then scaled such that for the simpler elastic model implemented in LIGGGHTS this induces the correct macroscopic stress field leading to fracture formation, see Fig. 1. Comparison to the spatial scales of crack patterns observed on the nucleus yields information on the material properties.

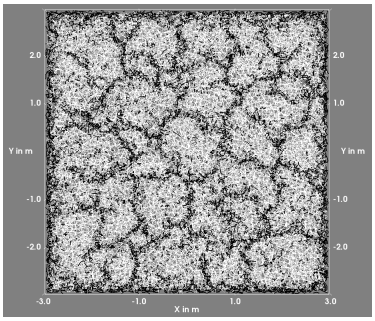

Figure 1: Top view of bond network (white) and broken bonds (black) forming a 1-m-scale crack pattern.

Acknowledgements

This work is part of the research project "The Physics of Volatile-Related Morphologies on Asteroids and Comets". DK, KO, NO, TM, and DH would like to gratefully acknowledge the financial support and endorsement from the DLR Management Board *Young Research Group Leader Program* and the Executive Board Member for *Space Research and Technology*.

References

[1] Kloss C. et al.: Prog. Comput. Fluid Dy., 12(2/3), 140–152, 2012.
[2] Potyondy D. O. and Cundall P. A.: Int. J. Rock Mech. Min., 41, 1329–1364, 2004.
[3] LIGGGHTS-WITH-BONDS, https://github.com/richti83/LIGGGHTS-WITH-BONDS.
[4] Bierwisch C. et al.: J. Mech. Phys. Solids, 57, 10–31, 2009.
[5] Vincent J.-B. et al.: Astron. Astrophys., 587, A14, 2015.
[6] Pajola M. et al.: Nature Astronomy, 1, 0092, 2017.
[7] Mottola S. et al.: Science, 349(6247), aab0232, 2015.
[8] Otto K. et al.: Asteroids, Comets, Meteors ACM2017, Montevideo, Uruguay, 2017.
[9] Auger A.-T. et al.: Icarus, 301, 173–188, 2018.
[10] Attree N. et al.: Astron. Astrophys., 610, A76, 2018.

EPSC Abstracts
Vol. 12, EPSC2018-800, 2018
European Planetary Science Congress 2018

Experimental Insights on the Densification of Regoliths by Thermal Cycling

I. S. Curren and O. Aharonson
Department of Earth and Planetary Sciences, Weizmann Institute of Science, Rehovot, Israel (*ivy.curren@weizmann.ac.il*)

Abstract

A range of processes are implicated in the formation and modification for planetary regoliths, but the individual contributions of each mechanism are unknown. In this work we investigate the role of thermal cycling, perhaps the most ubiquitous process occurring on airless bodies, in regolith evolution. We demonstrate experimentally that thermal cycling can cause granular compaction in unconsolidated granular materials, but that initially compact materials remain unmodified over the range of parameters tested. Our results tentatively suggest that thermal cycling induced regolith compaction will reach a saturation density (over a timescale determined by insolation parameters) that will remain unchanged unless by another modification process.

1. Introduction

Regoliths are a common feature on rocky and airless bodies. Consisting primarily of fragmented granular debris, they serve as the interface between space and the interior of a body. As such, they are continuously formed and modified by a range of frequent small-scale processes and infrequent large-scale events [1], the signatures of which are likely recorded in the regolith. Our current understanding of regolith evolution does not include individual inputs from modification processes, which hampers efforts to interpret remote sensing datasets that are sensitive to regolith properties.

Thermal cycling by insolation is advocated as one of the processes responsible for forming and modifying regoliths on rocky bodies [2-4]. The non-stochastic nature of this process makes it suitable for theoretical and laboratory testing, but few studies have investigated the effect of thermal cycling in the context of regolith evolution [4]. Here, we perform experiments examining the influence of thermal cycling on regolith simulant fines and other granular media.

2. Experimental Methods

We perform a suite of experiments to test the effects of thermal cycling on granular materials at the Simulated Planetary ICes and Environments Laboratory (SPICE Lab) at the Weizmann Institute of Science. Using a PID loop, we impose sinusoidal temperature variations on samples in a radial heating configuration. T-type thermocouples continuously monitor and log sample temperatures and a DSLR camera captures images at designated intervals, which are then used to analyze each experiment. We vary the cycle temperature range (ΔT), number of cycles (n_{cycles}), atmospheric pressure, sample material, sample container, and initial compaction state.

3. Results and Discussion

The experiments carried out in this study demonstrate several important concepts with respect to regolith compaction stemming from thermal cycling. First, we show that ΔT is positively correlated with the extent of densification of initially uncompact samples (Fig. 1), which is consistent with previous work [4-5]. Across the solar system and on a single body, ΔT can vary widely, dictated primarily by the object's topography and orbital parameters. Our results suggest that porosity may be observably higher in regions where the temperature fluctuations are small, such as in permanently shadowed craters on the Moon where water ice is known to persist [6].

We also demonstrate that the degree of compaction varies for dissimilar types of granular materials (Fig. 1). The thermal expansion and contraction of spherical granular materials have been shown to result in the reconfiguration of grains into more optimally packed arrangements [5]. In the case of planetary regoliths, which are often angular and irregularly shaped, it is possible to substantially alter the packing arrangement through this same process (Fig. 2). The significant density changes observed in our uncompacted regolith trials reflect this concept.

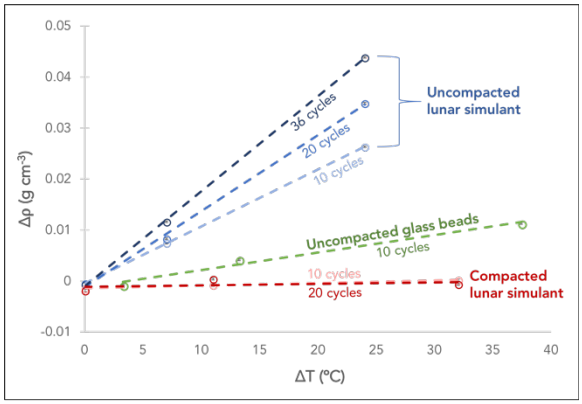

Figure 1: Change in density for thermally cycled materials over a range of temperatures and n_{cycles}. Dashed lines are linear fits to the data. Points at $\Delta T=0$ are control experiments with no temperature oscillations.

Experiments in initially uncompacted samples were also shown to increase in density with each progressive thermal cycle, although samples did not reach saturation density, similar to previous work [4-5]. Experiments with initially compacted (porosities approximately 10% lower than uncompacted samples) lunar regolith simulant showed no changes over twenty cycles for a range of temperatures (Fig. 1). We interpret this as an indication that these samples exceed the aforementioned saturation density and were not able to rearrange to a less dense matrix in the experimental conditions.

Density and grain connectivity is known to influence the thermophysical properties of regolith [7]. Examples of this can be seen on the Moon, around "cold spots," which are regions of low thermal conductivity surface soil surrounding recent impacts [7-8] that appear to fade over a 150 kyr timescale [9]. These features will act as a natural laboratory for future work as we incorporate experimental results into a comprehensive model for thermally induced changes in regolith.

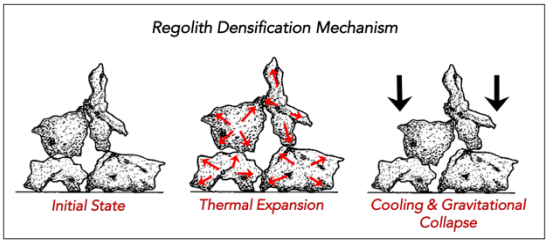

Figure 2: Cartoon of regolith densification via the thermal cycling mechanism. The irregular shapes of regolith permit significant changes in packing arrangement.

4. Summary and Conclusions

Thermal cycling of uncompacted regolith simulants and granular materials leads to sample densification that increases as a function of ΔT and n_{cycles}. Conversely, initially compact regolith simulants remain unchanged by the same thermal cycling process during the course of our experiments. We suggest this behavior implies that thermal cycling densification is irreversible by the same process. If regoliths are continuously approaching or reach their saturation density through this modification process, then the contribution of thermal cycling to regolith evolution may be modeled, estimated and validated with remote sensing datasets.

Acknowledgements

This work is supported in part by the Zuckerman STEM Leadership Program and the Feinberg Graduate School of the Weizmann Institute of Science.

References

[1] Wolman, M.G. and Miller, J.P.: Magnitude and Frequency of Forces in Geomorphic Processes, The Journal of Geology, Vol. 68, pp. 54-74, 1960. **[2]** M. Delbo, Libourel, G., Wilkerson, J., et al.: Thermal fatigue as the origin of regolith on small asteroids, Nature, V. 508, pp. 233-236, 2014. **[3]** Molaro, J.L., Byrne, S., and Le, J.-L.: Rates of temperature change of airless landscapes and implications for thermal stress weathering, Journal of Geophysical Research E: Planets, V. 117, E10 , 2012. **[4]** Gamsky, J., and Metzger, P.: The Physical State of Lunar Soil in the Permanently Shadowed Craters on the Moon, ASCE Conference on Earth and Space, pp. 14-17, 2010. **[5]** Chen, K., Cole, J., Conger, C., et al.: Granular Materials: Packing grains by thermal cycling, Nature, V. 442, pp. 257, 2006. **[6]** Spudis, P.D., Bussey, D.B.J., Baloga, S.M., et al.: Initial results for the north pole of the Moon from Mini-SAR, Chandrayaan-1 mission, Geophysical Research Letters, V. 37, no. 6, 2010. **[7]** Hayne, P., Bandfield, J., Siegler, M., et al.: Global Regolith Thermophysical Properties of the Moon From the Diviner Lunar Radiometer Experiment, Journal of Geophysical Research: Planets, V. 122, pp. 2371-2400, 2017. **[8]** Bandfield, Song, E., Hayne, P, et al.: Lunar cold spots: Granular flow features and extensive insulating materials surrounding young craters, Icarus, V. 231, pp. 221-231, 2014. **[9]** Williams, J.-P., and Bandfield, J.: Lunar cold spots and crater production on the Moon, AAS Division of Planetary Sciences Meeting #48, 16-21 October 2016, Pasadena, CA.

EPSC Abstracts
Vol. 12, EPSC2018-801, 2018
European Planetary Science Congress 2018

Thermal Inertia of Binary Near-Earth Asteroids

B. Rozitis (1), E. C. Brown (2), S. F. Green (1), S. C. Lowry (3), A. Fitzsimmons (4), A. Rozek (3), C. Snodgrass (1), P. Weissman (5) and T. Zegmott (3).
(1) The Open University, UK (benjamin.rozitis@open.ac.uk), (2) University of Oxford, UK, (3) University of Kent, UK, (4) Queens University Belfast, UK, (5) Planetary Science Institute, Arizona, USA.

Abstract

Binary asteroids represent approximately 15% of the near-Earth asteroid population, and their study can provide important insights into the physical processes that act on all asteroids. From thermophysical modelling of 7 binary near-Earth asteroids, we determined that their average thermal inertia value was 150 ± 50 J m^{-2} K^{-1} $s^{-1/2}$, which implies that small grains are preferentially kept during their formation.

1. Introduction

Approximately 15% of near-Earth asteroids are inferred to be binaries [1], and they represent an interesting and important asteroid sub-population to study. In particular, the presence of a satellite allows the mass and bulk density of a binary asteroid system to be determined through Kepler's laws after studying the secondary's orbit about the primary. By studying their orbital configurations, most binary asteroids have low bulk density values (i.e. ~1 to 2 g cm^{-3}) and high macro-porosity values (i.e. ~40-60 %), which implies that they are rubble-piles and not solid coherent bodies. Furthermore, the primaries within binary systems are also rapidly rotating (i.e. rotation periods of 2 to 4 hours), which gives strong insights into how they formed and the physical processes that affect all asteroids in general.

It is now generally accepted that most binary near-Earth asteroids are formed by YORP-induced rotational mass loss rather than by gravitational disruption during a close planetary encounter [2]. Light-curve and radar observations of binary asteroids reveal that the rapidly rotating primaries have a "spinning top" shape with a prominent equatorial ridge (e.g. 1999 KW4 is a classic example), and that the secondaries are on stable circular orbits about their primaries [3]. Numerical simulations of rubble-piles steadily spun-up by YORP demonstrate how mass gradually lost from a primary asteroid re-accumulates in a circular orbit about it to form a small secondary [2]. The shape deformation induced on the simulated primary produces a "spinning top" shape that strongly resembles that seen in radar observations of binary near-Earth asteroids.

At present, the numerical models do not specify what type of material is preferentially lost from the primary asteroid to form the secondary asteroid. If the primary asteroid has no cohesion then small regolith grains would be preferentially lost because the asteroid's gravity is less effective at holding onto them compared to larger regolith grains. This would then leave behind large regolith grains on the primary asteroid's surface. However, if the primary asteroid has a significant degree of cohesion then large regolith grains would be preferentially lost because cohesive forces are stronger for smaller regolith grains [4]. So, in contrast to the no-cohesion case, this would then leave behind small regolith grains.

To identify what regolith grain size is preferentially left behind on the primary asteroid surface, the thermal inertia of the asteroid's surface can be determined from thermal-infrared observations and thermophysical modelling. This is because thermal inertia (i.e. a material's resistance to temperature change) can be used as a qualitative measure of the regolith grain size (i.e. low and high thermal inertia values arise from small and large regolith grains, respectively). Previous work by [5] has used a distribution of 12 NEATM beaming parameters of 8 binary near-Earth asteroids to infer that their mean thermal inertia value was 480 ± 70 J m^{-2} K^{-1} $s^{-1/2}$. This is more than double the mean value of 200 ± 40 J m^{-2} K^{-1} $s^{-1/2}$ inferred in equivalent work for solitary near-Earth asteroids [6], and suggests that binary near-Earth asteroids preferentially have large regolith grains on their surfaces. However, our previous work involving full thermophysical modelling for 3 binary near-Earth asteroids, i.e. (1862) Apollo [7], (175706) 1996 FG3 [8], and (276049) 2002 CE26 [9], has found a much lower mean thermal inertia value of ~140 J m^{-2} K^{-1} $s^{-1/2}$, which instead suggests that small regolith grains are preferentially left on their surfaces. To resolve this apparent discrepancy, we measured

the thermal inertia values of an additional 4 binary near-Earth asteroids using thermal-infrared observations and thermophysical modelling, i.e. for (3671) Dionysus, (66391) 1999 KW4, (153491) 2001 SN263, and (185851) 2000 DP107 (see Table 1).

2. Thermal-IR Observations

We utilised archive NEOWISE data for (3671) Dionysus, NASA IRTF data for (153491) 2001 SN263, and Spitzer Space Telescope data for (185851) 2000 DP107 for the thermophysical modelling of those binary asteroids. Additionally, we obtained new observations of (66391) 1999 KW4 on 27th May 2016 using the VISIR instrument located on ESO's VLT telescope in Chile. The observations were obtained in imaging mode for wavelengths of 8.7-12.5 μm. The images were reduced using the VISIR image processing pipeline, and photometry was performed using standard techniques on the reduced images to give the measured asteroid fluxes.

3. Thermophysical Modelling

To determine the thermal inertia values of the 4 additional binary near-Earth asteroids studied, thermophysical modelling was performed using the ATPM [10] with their previously published shape models and pole orientations. In particular, the ATPM computes the surface temperature distribution of an asteroid by solving 1D heat conduction for each triangular facet of the asteroid shape model. A surface boundary condition is included for each facet that ensures conservation of energy between incoming radiation (i.e. direct solar illumination plus scattered light between facets), heat conducted into the sub-surface (i.e. dictated by thermal inertia), and radiated energy (i.e. thermal emission). Rough surface thermal-infrared beaming is also included by a fractional coverage of hemispherical craters. Model surface temperature distributions are produced for a range of thermal inertia values, and the model emitted flux is derived by summing the Planck function across facets visible to the observer. The model fluxes are then compared against the measured fluxes using χ^2 fitting to find the best-fit parameters and their uncertainties.

4. Summary and Conclusions

Based on the 7 asteroids studied in Table 1, the average thermal inertia value for a binary near-Earth asteroid was found to be 150 ± 50 J m^{-2} K^{-1} s$^{-1/2}$. This is at the lower end of the average value of 385 ± 225 J m^{-2} K^{-1} s$^{-1/2}$ determined for 12 solitary near-Earth asteroids via thermophysical modelling [11], and is significantly less than the previously reported value of 480 ± 70 J m^{-2} K^{-1} s$^{-1/2}$ [5]. This implies that fine-grained regolith is preferentially kept during the formation of binary asteroids by YORP spin-up.

Table 1: Summary of the binary near-Earth asteroids studied in this and previously published work.

Binary Asteroid	Spectral Type	Size (km)	Source
Apollo	Q	1.6	Reference [7]
Dionysus	C	1.1	This work
1999 KW4	S	1.3	This work
2001 SN263	B	2.5	This work
1996 FG3	C	1.7	Reference [8]
2000 DP107	S	0.9	This work
2002 CE26	C	3.5	Reference [9]

Acknowledgements

BR acknowledges support from the Royal Astronomical Society in the form of a research fellowship. Based on observations performed at the ESO Paranal Observatory in Chile (program ID 197.C-0816). Also based on data products from NEOWISE and the Spitzer Space Telescope, which are operated by the Jet Propulsion Laboratory/ California Institute of Technology under contracts with NASA.

References

[1] Pravec, P. and Harris, A. W.: Icarus, Vol. 190, pp. 250-259, 2007.
[2] Walsh, K. J. *et al.*: Nature, Vol. 454, pp. 188-191, 2008.
[3] Ostro, S. J. *et al.*: Science, Vol. 314, pp. 1276-1280, 2006.
[4] Scheeres, D. J. *et al.*: Icarus, Vol. 210, pp. 968-984, 2010.
[5] Delbo, M. *et al.*: Icarus, Vol. 212, pp. 138-148, 2011.
[6] Delbo, M. *et al.*: Icarus, Vol. 190, pp. 236-249, 2007.
[7] Rozitis, B. *et al.*: A&A, Vol. 555, id. A20, 2013.
[8] Wolters, S. D. *et al.*: MNRAS, Vol. 418, pp. 1246-1257, 2011.
[9] Rozitis, B. *et al.*: MNRAS, Vol. 477, pp. 1782-1802, 2018.
[10] Rozitis, B. and Green, S. F.: MNRAS, Vol. 415, pp. 2042-2062, 2011.
[11] Delbo, M. *et al.*: Asteroids IV, University of Arizona Press, pp. 107-128, 2015.

EPSC Abstracts
Vol. 12, EPSC2018-828, 2018
European Planetary Science Congress 2018

Fine-Grained Regolith on the Young Asteroids (1270) Datura and (5026) Martes

B. Rozitis (1), E. C. Brown (2), S. F. Green (1), S. C. Lowry (3), A. Fitzsimmons (4), A. Rozek (3), C. Snodgrass (1), P. Weissman (5) and T. Zegmott (3).
(1) The Open University, UK (benjamin.rozitis@open.ac.uk), (2) University of Oxford, UK, (3) University of Kent, UK, (4) Queens University Belfast, UK, (5) Planetary Science Institute, Arizona, USA.

Abstract

Regolith is found on most, if not all, solid planetary surfaces but its formation timescales are uncertain, especially on asteroids. To place constraints on these timescales, we characterised the surface properties of two "young asteroids" with estimated ages of <600 kyr. The two asteroids were observed in the thermal-infrared with the ESO VLT VISIR instrument, and thermal modelling of the data surprisingly found the presence of fine-grained regoliths on both asteroids.

1. Introduction

Space missions and remote sensing observations have shown that most, if not all, solid planetary surfaces are covered by a regolith layer, i.e. a surface layer comprised of centimetre-sized or smaller particles [1]. Regolith generation is believed to arise from micrometeorite impact gardening and fracturing by thermal fatigue [1]. Both processes require time to grind the regolith grains down to smaller sizes but the timescales involved are uncertain. However, it has been recently suggested that thermal fatigue should be the dominant mechanism for small asteroids [1].

Thermal inertia (i.e. a material's resistance to temperature change) can be used as a qualitative measure of the regolith grain size (i.e. low and high thermal inertia values arise from small and large regolith grains, respectively) [2], and can be determined through thermophysical modelling of suitable thermal-infrared observations [3]. Such observations and models have successfully been applied to a range of Solar System bodies to infer their likely regolith grain sizes (e.g. see [2] and [3] for a brief review). For the lunar surface, LRO Diviner observations and modelling have shown that the thermal inertia values of impact ejecta surrounding lunar craters are related to the estimated ages of those craters (i.e. determined by crater counting) [4]. In particular, older craters are surrounded by impact ejecta with lower thermal inertia values than that surrounding younger craters, and confirms that time is needed on the lunar surface to grind the regolith grains down to smaller sizes.

For asteroids, a previously identified trend of decreasing thermal inertia with increasing asteroid size was thought to be related to the relative ages of those asteroids because larger asteroids are generally older than smaller asteroids [5]. However, recent work has demonstrated that this apparent size trend could be a manifestation of temperature-dependent thermal inertia, and that this size trend can be reduced/removed when the asteroid thermal inertia measurements are corrected to a common heliocentric distance [6]. Therefore, it is not clear what timescales are needed for regolith generation on asteroid surfaces.

Fortunately, asteroid families and unbound asteroid pairs allow the ages of their member asteroids to be determined through backwards dynamical integrations [7]. Therefore, they can be used to place chronological constraints on asteroid regolith generation if their thermal inertia values are also measured. Two suitable "young asteroids" with well-constrained dynamical ages are the main-belt asteroids (1270) Datura and (5026) Martes, which we investigate in this work with ESO VLT VISIR observations and thermophysical modelling.

2. (1270) Datura and (5026) Martes

(1270) Datura is the largest member of a small asteroid family (i.e. 17 currently known members) located in the innermost part of the main asteroid belt [8]. This collisionally produced family has an estimated age of 450 to 600 kyr, and its members consist of S and Q type sub-classes. (5026) Martes is the largest member of an unbound asteroid pair (i.e. its counterpart asteroid is 2005 WW113), and has an estimated separation age of just 18 kyr [9]. It has a C-

type spectral class. Both (1270) Datura and (5026) Martes have previously derived light-curve shape models [8][9].

3. ESO VLT VISIR Observations

We observed (1270) Datura and (5026) Martes in May and April 2016, respectively, with the VISIR instrument located on ESO's VLT telescope in Chile (see Table 1). The thermal-infrared observations were obtained in imaging mode, and standard star observations were conducted at airmasses that bracketed the asteroid observations. The images were reduced using the VISIR image processing pipeline, and photometry was performed using standard techniques on the reduced images to give the measured asteroid fluxes.

Table 1: Summary of ESO VLT VISIR observations obtained in 2016.

Asteroid	Date	r (AU)	Δ (AU)	α (°)	Wavelengths (μm)
Datura	27/5	2.2	1.2	10	8.7, 10.7, 11.5, 12.5
Martes	10/4	2.2	1.5	21	8.7, 11.5

4. Thermophysical Modelling

To determine the thermal inertia values of (1270) Datura and (5026) Martes, thermophysical modelling was performed using the ATPM [10] with the previously derived light-curve shape models. In particular, the ATPM computes the surface temperature distribution of an asteroid by solving 1D heat conduction for each triangular facet of the asteroid shape model. A surface boundary condition is included for each facet that ensures conservation of energy between incoming radiation (i.e. direct solar illumination plus scattered light between facets), heat conducted into the sub-surface (i.e. dictated by thermal inertia), and radiated energy (i.e. thermal emission). Rough surface thermal-infrared beaming is also included by a fractional coverage of hemispherical craters. Model surface temperature distributions are produced for a range of thermal inertia values, and the model emitted flux is derived by summing the Planck function across facets visible to the observer. The model fluxes are then compared against the measured fluxes using χ^2 fitting to find the best-fit parameters and their uncertainties. Table 2 summarises the ATPM fitting results of the VISIR data for (1270) Datura and (5026) Martes.

Table 2: Summary of thermophysical properties derived by the ATPM.

Asteroid	Size (km)	Geometric Albedo	Thermal Inertia ($J\ m^{-2}\ K^{-1}\ s^{-1/2}$)
Datura	7.5	0.27	20 ± 5
Martes	10.7	0.04	40 ± 30

5. Summary and Conclusions

The low thermal inertia values determined for (1270) Datura and (5026) Martes imply that both asteroids are covered by fine-grained regoliths. Furthermore, their thermal inertia values are comparable to that measured for several main-belt asteroids that are much larger [3]. This could imply that the regolith generation processes take place on timescales much shorter than previously thought, as suggested by [6]. Alternatively, the fine-grained regoliths could be related to the formation mechanisms of the asteroids themselves, i.e. a catastrophic collision for (1270) Datura and YORP spin-up/rotational fission for (5026) Martes. Further observations and modelling of asteroids with known ages will help place additional constraints on the regolith generation timescales.

Acknowledgements

BR acknowledges support from the Royal Astronomical Society in the form of a research fellowship. Based on observations performed at the ESO Paranal Observatory in Chile (program ID 197.C-0816).

References

[1] Delbo, M. *et al.*: Nature, Vol. 508, pp. 233-236, 2014.
[2] Gundland, B. and Blum, J.: Icarus, Vol. 223, pp. 479-492, 2013.
[3] Delbo, M. *et al.*: Asteroids IV, University of Arizona Press, pp. 107-128, 2015.
[4] Hayne, P. O. *et al.*: Journal of Geophysical Research: Planets, Vol. 122, pp. 2371-2400, 2017.
[5] Delbo, M. *et al.*: Icarus, Vol. 190, pp. 236-249, 2007.
[6] Rozitis, B. *et al.*: MNRAS, Vol. 477, pp. 1782-1802, 2018.
[7] Pravec, P. *et al.*: Nature, Vol. 466, pp. 1085-1088, 2010.
[8] Vokrouhlický, D. *et al.*: A&A, Vol. 598, id. A91, 2017.
[9] Polishook, D.: Icarus, Vol. 241, pp. 79-96, 2014.
[10] Rozitis, B. and Green, S. F.: MNRAS, Vol. 415, pp. 2042-2062, 2011.

EPSC Abstracts
Vol. 12, EPSC2018-1056, 2018
European Planetary Science Congress 2018

A code for the study of gravitational aggregates with non-spherical particles

Fabio Ferrari, Michèle Lavagna
Politecnico di Milano, Milano, Italy, (fabio1.ferrari@polimi.it)

Abstract

A recently popular way to study the internal properties and structure of "rubble pile" asteroids is to study them as gravitational aggregates, through numerical N-body simulations. These methods are suitable to reproduce aggregation scenarios after disruption and allow the study of the dynamical and collisional evolution of fragments up to the formation of a stable aggregate or to their dispersion. This work presents a numerical implementation of the gravitational N-body problem with contact dynamics between non-spherically shaped rigid bodies. The work builds up on a previous implementation of the code and extends its capabilities. The number of bodies handled is significantly increased through the use of a CUDA/GPU-parallel octree structure. The main features of the code are described and its performance are compared against CPU-parallel architectures and classical direct N^2 integration. Preliminary results and examples of scenarios that could benefit from such implementation are presented, with application to asteroid gravitational aggregation problems.

1. Introduction

The study of aggregation phenomena mostly relies on codes optimized for a large number of mutually interacting particles, including parallel N-body tree codes [9, 13, 12, 11], hybrid codes [1], adaptive algorithms of optimal orders [10], systolic algorithms [5], or more generally symplectic codes [14, 6, 4]. These handle a large number of particles regardless of their individual shape and rigid body motion. Although not relevant for many applications, this limitation could be relevant for the case of asteroids [8], as suggested by results of granular dynamics in terrestrial engineering applications. The latter are commonly studied using multi-body codes, able to simulate contact interactions between a large number of complex-shaped bodies, but not suitable for gravitational dynamics. The code presented here is developed to joint the advantages of both classes of codes into a single implementation, to reproduce N-body gravitational dynamics between a large number of complex-shaped rigid bodies.

2. Numerical implementation

This work builds on a previous implementation of the code [7] and extends its capabilities by including a parallel CUDA-GPU octree structure. The following paragraphs briefly summarize the main features of the code.

2.1. Contact dynamics

Concerning collision and contact dynamics, the N particles are treated as three-dimensional rigid bodies of arbitrary shape. Each body possesses rotational degrees of freedom, a tensor of inertia and a mesh to be used for collision detection. In our implementation, bodies can collide and re-bounce in collision types ranging from fully elastic to complete inelastic, depending on the selected restitution coefficient. Because we assume the rigid nature of bodies, contact forces are discontinuous and lead to a non-smooth constraint-based problem. In addition, the code provides the choice to select smooth penalty-based (soft-body) contact solver, which is best suited for high velocity impact dynamics. The interested reader can refer to [7] for further details.

2.2. GPU-parallel octree structure

Compared to direct N-body integrators, algorithms based on tree data structures rely on more dynamic and adaptive computations that allow for a significant reduction of time complexity from $O(N^2)$ up to $O(N\ \log(N))$. Our code implements the Barnes-Hut algorithm [2], which groups particles using a hierarchy of cube structures. A node in the algorithm corresponds to a cube in physical space. Because of the use of octrees, each node has eight child nodes obtained by a simple homogeneous spatial subdivision performed along the three principal axis of the system. The

tree is therefore built by recursive sub-division until each node of the tree contains zero or one particle. The structure is adaptive, implying that the size of the tree is not fixed but comes as a result of the repartition of the particles in the 3D space.

The implementation of the Barnes-Hut algorithm on a GPU using CUDA language is inspired by the work of Burtscher and Pingali [3]. The physical domain is divided into sub-domains and the bodies are grouped following the octree structure. The numerical tasks to follow the Barnes-Hut algorithm have been divided among five kernels, to be executed sequentially on the GPU.

3. Numerical simulations

Numerical simulations are performed under many degrees of freedom. To reproduce asteroid aggregation scenarios, it is important to carefully select the physical properties of the N bodies and their initial dynamics. Initial conditions play a crucial role to the formation of the aggregates and their properties. As mentioned, bodies are modeled as complex-shaped bodies and their initial dynamical state includes relative position and velocity of their center of mass, angular position and spin rate. Other relevant simulation parameters include integration time step, to be chosen according to the characteristic time of dynamics [7]. These include gravitational dynamics (slow) and contact/collision dynamics (fast). Due to a more restrictive requirement, the latest drive the selection of the time step, which is tuned according to the fastest dynamics of the system. The number of bodies (10^4 in our simulations), their characteristic size and maximum initial distance between them are also key aspects. The physical properties of fragments (density and surface properties) are also to be chosen. Figure 1 shows an example of aggregation process.

4. Summary and Conclusions

The work presents a GPU-parallel numerical code for the study of collisional and gravitational evolution of "rubble pile" asteroids. At this preliminary stage, the code is able to handle up to 10^4 complex-shaped interacting bodies. Preliminary results on scenarios simulated are very promising and hint a good capability of the code to reproduce asteroid aggregation scenarios.

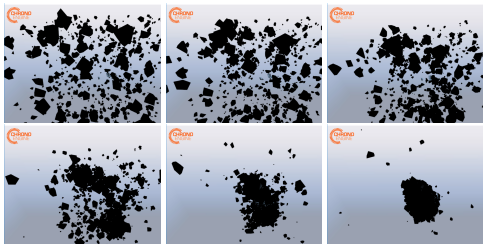

Figure 1: Aggregation sequence example with 1000 bodies

Acknowledgements

This project has received funding from the European Union's Horizon 2020 research and innovation programme under the Marie Skłodowska-Curie grant agreement No 800060.

References

[1] S. J. Aarseth. Nbody2: A direct n-body integration code. *New Astronomy*, 6:277–291, 2001.

[2] J. Barnes and P. Hut. A hierarchical o(n log n) force-calculation algorithm. *Nature*, 324:446–449, Dec. 1986.

[3] M. Burtscher and K. Pingali. Chapter 6 - an efficient cuda implementation of the tree-based barnes hut n-body algorithm. In W.-m. W. Hwu, editor, *GPU Computing Gems Emerald Edition*, Applications of GPU Computing Series, pages 75 – 92. Morgan Kaufmann, Boston, 2011.

[4] J. E. Chambers. A hybrid symplectic integrator that permits close encounters between massive bodies. *Monthly Notices of the Royal Astronomical Society*, 304:793–799, 1999.

[5] E. N. Dorband, M. Hemsendorf, and D. Merritt. Systolic and hypersystolic algorithms for the gravitational n-body problem, with an application to brownian motion. *Journal of Computational Physics*, 185:484–511, 2003.

[6] M. J. Duncan, H. F. Levison, and M. H. Lee. A multiple time step symplectic algorithm for integrating close encounters. *Astronomical Journal*, 116:2067–2077, 1998.

[7] F. Ferrari, A. Tasora, P. Masarati, and M. Lavagna. N-body gravitational and contact dynamics for asteroid aggregation. *Multibody System Dynamics*, 39(1):3–20, 2017.

[8] P. Michel, W. Benz, and D. C. Richardson. Catastrophic disruption of asteroids and family formation: a review of numerical simulations including both fragmentation and gravitational reaccumulations. *Planetary and Space Science*, 52(12):1109 – 1117, 2004. Catastrophic Disruption of Small Solar System Bodies.

[9] A. Morbidelli. Modern integrations of solar system dynamics. *Annual Review of Earth and Planetary Sciences*, 30(1):89–112, 2002.

[10] C. D. Pruett, J. W. Rudmin, and J. M. Lacy. An adaptive n-body algorithm of optimal order. *Journal of Computational Physics*, 187:298–317, 2003.

[11] D. C. Richardson, P. Michel, K. J. Walsh, and K. W. Flynn. Numerical simulations of asteroids modelled as gravitational aggregates. *Planetary and Space Science*, 57:183–192, 2009.

[12] D. C. Richardson, T. Quinn, J. Stadel, and G. Lake. Direct large-scale n-body simulations of planetesimal dynamics. *Icarus*, 143(1):45 – 59, 2000.

[13] J. Stadel. *Cosmological N-body simulations and their analysis*. PhD thesis, University of Washington, Seattle, WA, USA, 2001.

[14] J. Wisdom and M. Holman. Symplectic maps for the n-body problem. *Astronomical Journal*, 102:1528–1538, 1991.